
Faculty of Engineering

Faculty Publications

This is a post-print version of the following article:

Correlation of electrical conductivity, compressive strength, and permeability of repair materials

Boyu Wang & Rishi Gupta

March 2020

The final publication is available at:

<https://doi.org/10.14359/51722396>

Citation for this paper:

Wang, B., & Gupta, R. (2020). Correlation of electrical conductivity, compressive strength, and permeability of repair materials. *ACI Materials*, 117(2), 53-63.
<https://doi.org/10.14359/51722396>.

CORRELATION OF ELECTRICAL CONDUCTIVITY, COMPRESSIVE STRENGTH, AND PERMEABILITY OF REPAIR MATERIALS

Boyu Wang^a, Rishi Gupta^{b*}

^a Graduate Student, Department of Civil Engineering, University of Victoria, 3800 Finnerty Road, Victoria, B.C., V8W 2Y2, CANADA

^b Associate Professor, Department of Civil Engineering, University of Victoria, 3800 Finnerty Road, Victoria, B.C., V8W 2Y2, CANADA

* Corresponding author, Tel +1 (250)721-7033, email guptar@uvic.ca

Biography:

ACI member **Boyu Wang** is a PhD student at the University of Victoria, Victoria, B.C., Canada. He received his master's degree in mechanical engineering from University of Victoria in 2018. His research interests include NDT methods for evaluating concrete durability, concrete repair techniques, and fiber reinforced concrete.

ACI member **Rishi Gupta** is an Associate professor at the University of Victoria, Victoria, B.C., Canada. He received both his MASc and PhD in civil engineering from the University of British Columbia. He has more than 15 years of combined academic and industry experience in the field of Civil (Materials) Engineering. Rishi is a Fellow of Engineers Canada and is actively involved in several ACI Committees including 544 (Fiber Reinforced Concrete), ACI 59 (International Advisory Committee), and E803-01(Faculty Network). His research area covers hybrid fiber reinforced concrete, structural health monitoring, smart "self-sealing" materials, and innovative construction technologies.

ABSTRACT

In recent years, the construction industry has invested a lot of effort in increasing concrete safety and in extending the service life of structures. Several test methods, such as water penetration, surface/bulk electrical resistivity, rapid chloride permeability (RCP), and half-cell potential, have been proposed to study concrete durability. This study establishes the relationship between multiple durability test methods in the context of concrete repair, which was rarely selected as the object for study. By means of experimental study, this study finds that surface resistivity has a linear relation to bulk resistivity and a polynomial relation to water permeability. No relationship can be established between concrete resistivity and compressive strength, though high-strength concrete tends to have a high resistivity. RCP test results do not correlate well with resistivity measurements, which requires further study to overcome its heating and binding effect when measurements are being taken.

Keywords: Permeability, electrical resistivity, compressive strength, Half-cell potential, correlation analysis

INTRODUCTION

Concrete repair has become one of the hot topics in the civil engineering domain lately since structures around the world have almost reached the service limit where significant measure must be taken to maintain their safety and functionality. According to the Canadian Infrastructure report 2016 [1], the reinvestment rate of bridges is at 0.8%, about 165 million dollars, and the durability of the concrete repair is considered the deciding factor which affects how frequently the structures need to be repaired and thus how much money will be spent in

terms of material usage, labor, downtime, etc. Chloride ingress has been considered a major cause for rebar corrosion and repair delamination because the chloride can serve as the catalyst and initiate corrosion even if the alkalinity of the pore solution does not drop. Several methods have been proposed to study the ease with which aggressive ions can penetrate concrete including water permeability, rapid chloride permeability, surface/bulk electrical resistivity, half-cell potential, etc. Among most of the durability evaluation methods, surface resistivity has received favorable attention due to advantages such as ease of use, quick measurements, and less heating effect [2]. A great deal of work was done by previous researchers to correlate surface resistivity and other durability factors, such as water permeability, rapid chloride permeability, and mechanical properties.

Surface Resistivity vs. Compressive Strength

Although compressive strength does not indicate the durability of materials, many people have observed that compressive strength increased with the electrical resistivity of concrete samples over time. Some researchers have built both empirical and theoretical models given the similarities in the time development of both compressive strength and electrical resistivity [3]. Based on experimental results, empirical relationships including linear [2]–[5], power [6], [7], and exponential [8] fitted curves were built by the previous researcher to correlate strength and resistivity. However, the goodness of the fit calculated by different researchers varies significantly with R^2 values ranging from 0.4131 to 0.9826 (as summarized in Table 1), which led to contradictory conclusions. Multiple authors [2], [5] have also reported that the data points tended to scatter more if specimens with relative dissimilar properties were involved. Several researchers have attempted to explain the potential causes for the discrepancy in their different R^2 , and the most mentioned factors that could possibly lead to poor correlation include

interfacial transition zone (ITZ), the chemical compound of pore solution, and pore structures and geometry, whereas none of them have been widely accepted.

Surface Resistivity vs. RCP

Similarities can be found between surface resistivity and RCP methods. Surface resistivity can be acquired by applying alternating current to concrete and measure the corresponding voltage drop, inversely the RCP method applies a direct voltage and measures the averaged current passed. Therefore, it is reasonable to believe both methods are potentially interrelated, and in some way represent the resistivity/conductivity of concrete specimens, although RCP results mainly reveal the resistance to chloride penetration. So far, several researchers have reported a good correlation between resistivity and RCP, and empirical equations, power [2], [6], [7], linear [4], and exponential [8] equations, have been established with R^2 values ranging from 0.8922 to 0.99 (summarized in Table 1). Furthermore, a theoretical model has been proposed by Layssi et al. [9] that total electrical charge and resistivity can be related by equating the resistance value calculated from RCP and resistivity measurements, as shown in Eq. 1.

$$Q = I_{rcp} \cdot t = \frac{V_{rcp}}{\frac{L}{A} \cdot \rho} \cdot t = \frac{V_{rcp} \cdot A \cdot t}{L_{rcp}} \cdot \frac{1}{\rho_{bulk}} \quad (1)$$

where,

I and V are the electrical current and voltage respectively; t indicates the time duration of the RCP test; ρ indicates concrete resistivity; A represents the cross-sectional area and L indicates concrete specimen length; Q is the cumulative electrical charge in coulombs; The subscripts, such as rcp and bulk, represent the results from RCP and bulk resistivity tests respectively.

1 However, the empirical equations mentioned above are based on several uncertainties which
2 compromise their applicability to situations where different materials are used. Azarsa et al.
3 [4] reported the relationship established on 28-day-cured specimens disappeared when the
4 specimens at 56 days were used. Julio-Betancourt and Hooton [10] found the nonlinear
5 relationships established between conductivity and the electrical charge may be misleading due
6 to the strong heating effect of RCP test, and a linear relationship should be closer to reality if
7 the temperature during RCP test remains constant.

9 **Surface Resistivity vs. Water Permeability**

10 Permeability is evaluated by measuring the depth of water penetration under pressure and
11 Darcy's law is commonly used to quantify the permeability by evaluating the coefficient of
12 permeability. Ramezaniapour [2] reported the power relationship between water penetration
13 depth and surface resistivity with increasing R^2 values when specimens with the same type of
14 cementitious materials were used. This phenomenon was described in that the result of surface
15 resistivity depends on both microstructure and pore solution of concrete while water
16 penetration test depends only on microstructure. Furthermore, an exhaustive study has been
17 conducted on the factors that affect water permeability of concrete including w/c ratio [11],
18 fine and coarse aggregates content [12], [13], pore structures [14], and ITZ [15]. In comparison,
19 the factors that affect surface resistivity include w/c ratio, aggregate size and type, and curing
20 conditions [16]. It is understandable that some common factors, such as w/c, aggregate size
21 and type, and pore microstructures form the fundamental relationship between surface
22 resistivity and water permeability. However, by summarizing the materials used by previous

1 researchers, insufficient work was done using concrete repair materials, which may have
2 different pore structure especially when polymers are added.

3
4 In summary, most of the previously established correlations were based on experimental data
5 obtained from conventional concrete, whereas repair materials were rarely selected as the
6 object for study. Repair materials are made to have high early-strength and better durability so
7 that chemical and mechanical properties may differ from conventional concrete. In addition,
8 surface resistivity was regarded as an alternative to RCP method and was found to correlate
9 well with other durability parameters and compressive strength, but some researchers also
10 reported their poor correlations in some cases. Therefore, the aim of this study is to provide
11 more evidence on revealing factors that affect their relationships and to establish correlations
12 between surface resistivity and other durability factors when repair materials are used. The
13 correlations based on repair materials will be compared with those obtained from conventional
14 concrete, and the mechanism behind the relationship of durability performance results will be
15 further explored.

17 **RESEARCH SIGNIFICANCE**

18 The findings from this study will be useful to assess the feasibility of applying the previously
19 established correlations based on ordinary concrete results to repair materials. Also, this study
20 will aid in revealing the mechanism behind the relationships of different durability factors.
21 Since concrete repair is typically expensive and labor-intensive, it is prudent to select a long-
22 lasting and durable repair material. Therefore, this research will also help bridge the knowledge
23 gap in regard to selecting suitable repair materials for different environmental conditions.

EXPERIMENTAL INVESTIGATION

Materials

Three types of commercially available cement-based repair materials are used and termed as Mix F, M, and P in this paper. The three mixes are offered as ready to use products in 25 kg (Mix F and Mix M) and in 22.7 kg (Mix P) bags. They are mixed with water to achieve the desired consistency, and the fresh properties of the materials are evaluated, as shown in Table 2. Mix F (cementitious repair concrete) has a maximum aggregate size of 9.5mm. Since the coarse aggregate size of Mix F is relatively small, durability test results of Mix F are compared with those of the other two repair mortars. In this study, samples of each mix are prepared using the water/materials ratio (w/m) as per manufacturers' specifications.

Specimens

Concrete cylinders with a dimension of 4-inch (100-mm) diameter and 8-inch (200-mm) length were cast for compressive strength, surface resistivity, and bulk resistivity tests following ASTM C39 [17], AASHTO TP95 [18], and ASTM C1760 [19] respectively. Some of these specimens were sliced into 2-inch (50-mm) concrete disks for RCP tests using a wet tile saw. Cylinders of 6-inch (150-mm) diameter and 6-inch (150-mm) length were cast for water penetration test, and 6-inch (150-mm) by 6-inch (150-mm) by 21-inch (533-mm) prisms were produced for half-cell measurements. It should be noted that concrete prisms were reinforced with steel bars (with a diameter of 10 mm) located at a 0.5-inch (12.7-mm) and one-inch (25-mm) distance away from the prism bottom, so as to study how cover depth affects the corrosion rate of reinforcements.

Methods

The multiple test methods used in this study can be classified into four categories based on the properties that these methods are measuring. The measured material properties include electrical conductivity, permeability, compressive strength, and corrosion potential. Concrete electrical conductivity reveals the ease with which electrical current passes through the concrete and defines the rate of corrosion of the rebar. Concrete permeability is affected by parameters including total porosity, connectivity, and tortuosity of concrete pores, and is related to the electrical conductivity, compressive strength, and corrosion potential. Corrosion potential is a voltage difference built up between the anodic and cathodic areas on the rebar and can also affect the rate of corrosion of the rebar.

Surface Electrical Resistivity

Surface resistivity is a well-established procedure for detecting surface resistivity as per AASHTO TP95. The four-point Wenner probe has been widely used for this test, whose schematic is demonstrated in Fig. 1(a). In our study, Giatec SurfTM apparatus was employed for resistivity measurement, as shown in Fig. 1(b). As seen, the sample holder has four sets of electrodes, placed at 90-degree array. Before the experiment, probe distance (denoted “a”) was adjusted to be 1.5 inches (38 mm) and the electrical current frequency was set to 13 Hz in accordance with AASHTO TP95. Once the test started, the apparatus ran two rounds so that eight measurements were taken and then averaged to obtain the resistivity around the test specimen.

The surface resistivity test was performed on specimens every 14 days after 28 days of water curing up to 70 days of curing. These specimens were then immersed in the sodium chloride

1 solution with a concentration of 35 parts per thousand (ppt) for another 14 and 28 days to
2 simulate conditions experienced by concrete repair in marine applications.

4 **Bulk Electrical Resistivity**

5 In bulk resistivity measurement, the test mechanism is demonstrated in Fig. 2(a) and the
6 corresponding test setup is shown in Fig. 2(b). Specimens were taken from the curing tank just
7 before the test started and surface water was blotted off in order to achieve the saturated surface
8 dry condition (SSD). The concrete specimen was placed between two parallel metal plates
9 which were connected to an alternating current source. Additionally, a wet sponge was
10 sandwiched between the concrete specimen and the metal plate to maintain the electrical
11 continuity during the test. The frequency of electrical current was set 1 kHz during the test
12 because high frequency can eliminate the polarization effect when measuring the resistance of
13 concrete specimens. Bulk electrical resistivity tests were conducted on 90-day samples cured
14 in tap water at 23 plus or minus two degrees Celsius.

16 **Rapid Chloride Permeability**

17 The RCP test was conducted on 28-day water-cured samples following ASTM C1202 [20]. A
18 60-volt DC potential was maintained across the specimen for 6 hours during which the
19 electrical current passed was recorded. The current value was then integrated with respect to
20 time to obtain the cumulative electrical charge which quantifies the chloride ion penetrability
21 of the specimens. The test setup is shown in Fig. 3.

23 **Water permeability**

Water permeability was measured on water-cured samples at 28 days using a water penetration apparatus as per standard DIN 1048. As shown in Fig. 4(a), a nitrogen gas tank was connected to the apparatus to apply pressure on the specimen bottom surface with a pressure value of 5 bar (0.5 MPa). This pressure was maintained for 72 hours, after which specimens were split into two halves by means of the direct tensile test. As shown in Fig. 4(b), the cylindrical specimen is placed on its side and loaded with diametral compression so as to induce transverse tension. The water penetration profile was then marked and used to calculate the coefficient of permeability which indicates the resistance to water penetration of concrete samples. The coefficient of permeability can be calculated using water penetration results. According to Darcy's Law, the depth of penetration can be expressed as:

$$\frac{dx}{dt} = k_w \frac{h}{x} \quad (2)$$

where x represents the depth of penetration (m), t indicates the experiment time (s), h is the water head (m), k_w is the coefficient of permeability. By integrating the equation and plugging in the initial condition, that is,

$$x(t=0)=0 \quad (3)$$

the k_w can be obtained as shown below:

$$k_w = \frac{x_w^2}{2ht} \quad (4)$$

where, x_w represents the maximum depth of water penetration. After splitting the specimen, the maximum depth of water penetration can be obtained as shown in Fig. 5. The test details

of permeability and RCP, as well as the corresponding experimental data, can be referred to Wang et al [21].

Compression Test

Concrete test specimens for compressive strength and bulk/surface electrical resistivity tests were demolded 24 hours after casting, and water cured in the curing chamber at 23 plus or minus two degrees Celsius until the testing day. Compression test was performed on 1-, 3-, 7-, 28-, and 70-day specimens in accordance with ASTM C39.

Half-cell Potential Test

The half-cell potential test was conducted on reinforced concrete prisms with a dimension of 6 inches (152.4 mm) by 6 inches (152.4 mm) by 21 inches (533.4 mm). After the specimens were demolded, they were immersed in tap water for 70 days, then in the simulated seawater with 35ppt salinity at ambient temperature for 28 days, and simulated seawater with 35ppt salinity at 60 degrees Celsius for 14 days. Additionally, these samples were left in an open space in BC Victoria for around one year before the test. Fig. 6 shows the schematic of the half-cell potential measurement setup. The copper/copper sulphate probe was used as the reference electrode and placed at the bottom of the specimens with a cover thickness of 0.5 inch (12.7 mm) and one inch (25.4 mm). The measurements were taken on the bottom surface in a two by four grid for a total of 8 test points, following the ASTM C876 [22]. It should be noted that half-cell potential was measured one year after sample casting and specimens were treated with chloride solution at ambient and elevated temperatures. The curing conditions of RCP, surface resistivity (SR), bulk resistivity (BR), water penetration (WP), compression, and half-cell potential test methods are summarized in Table 3.

EXPERIMENTAL RESULTS AND DISCUSSION

Electrical Resistivity and Compressive Strength Versus Curing Time

Fig. 7 (a) shows the development of surface resistivity of three mixes from 28 days to 98 days. Before the specimens were placed into the simulated seawater, all three mixes experienced a monotonical increase in resistivity from 28 to 70 days of curing, with Mix M having the highest percentage of increase (196%), followed by Mix P (68.4%) and Mix F (62.7%). Cementitious concrete (Mix F) and cementitious mortar (Mix M) revealed similar resistivity performance at 70-day ages, while the polymer-modified cementitious mortar (Mix P) only possess almost half the resistivity of the other two mixes.

As shown in Fig. 7 (b), compressive strength results of specimens with 1-, 3-, 7-, 28-, and 70-day curing in water were obtained as well as the results of specimens immersed in simulated seawater for additional 14 days after 70-day normal curing. As illustrated in Fig. 7 (b), all specimens gained strength during the initial curing stage. After 70 days of immersion, both Mix F and Mix M experienced a decrease in compressive strength, but Mix P increased slightly. It is a common belief throughout the construction industry that after 28 days of curing, concrete can reach almost 100% of its strength. But depending on mix design or the hydration rate of the constituent, strength of concrete after 28 days of curing can still increase such as Mix P in the case of this study. However, the measured concrete strength can be sensitive to environmental temperature and humidity as well as the degree of water saturation of concrete while tests were conducted. The strength reduction of Mix F and M may be affected by the aforementioned factor, and thus more test results for these two mixes are required. Additionally, as shown in Fig. 7 (b), all three materials experienced a decrease in strength after 14 days of immersion in simulated seawater. Compared to steel-reinforced concrete, the effect

of chloride ingress on the plain concrete specimen is relatively hard to predict. Shi et al. [57] reported that the strength of their mixes reacted differently (increase and decrease) to continuous sodium chloride immersion. By using a scanning electron microscope (SEM) and conducting an Energy-dispersive X-ray spectroscopy (EDX) analysis, it was found that chloride ions can chemically react with the cement hydrates and form new products in the concrete matrix. In this study, the newly formed product after the chloride solution immersion seemed to decrease the compressive strength of repair materials.

In general, the strength of concrete is defined by the strength of the cement paste and of the bonding between the paste and the aggregates. And it is widely believed that bond strength is largely dependent upon the ITZ where the properties of the cement paste are different than the paste far away from the physical interface, in terms of morphology, composition, and density. ITZ usually has less crack resistance and thus can result in the weak aggregate-paste link so fracture occurs preferentially in this place [23]. Therefore, in order to better understand the strength reduction of our specimens due to chloride ingress, further research is required to investigate the chemical composition changes in both cement paste and ITZ before and after chloride immersion.

Relationship Between RCP and Resistivity

Results of RCP and surface resistivity are summarized and plotted in Fig. 8 along with the fitted curves from previous researchers. It can be observed that the test results of Mix P and Mix M have a close agreement with results from previous literature by Ramezani-pour et al. [2] and Jackson [7], respectively. However, the results of Mix F (cementitious repair concrete) do not conform to any of the previously reported regression curves. The main difference stems

1 from the high surface resistivity and RCP results Mix F possessed. Normally, surface resistivity
2 values should be inversely proportional to the RCP results. As a result, no correlation function
3 between resistivity and RCP can be established in this study. As shown in Fig. 8, Mix F has
4 surface resistivity readings of around $60 \text{ k}\Omega \cdot \text{cm}$ and RCP values of around 2700 Coulombs,
5 which is almost three times the RCP values (around 1000 Coulombs) of other cementitious
6 concrete having similar resistivity results. Therefore, it is suspected that Mix F may be
7 especially susceptible to chloride penetration. In order to validate this, samples having cured
8 in water for 70 days were immersed in saltwater and tested using resistivity method. As shown
9 in Fig. 7 (a), a significant drop in surface resistivity for Mix F samples can be observed after
10 chloride exposure. It is believed that the presence of chloride ions significantly reduces the
11 resistivity of the Mix F.

12
13 There could be several reasons for Mix F's vulnerability to chloride penetration. Yuan et al.
14 [24] reported that chloride ions can either chemically or physically bind to hydration products.
15 The chloride binding to cement-based material was found to be a complicated process, which
16 could be influenced by chloride concentration, cement composition, supplementary
17 cementitious materials, etc. Therefore, materials with low binding capability to chloride ions
18 can lead to high chloride penetration. Heating effect during RCP test could be another
19 important reason. Due to the high voltage (60 volts) imposed on the specimens, temperature
20 rise seems inevitable during RCP measurements. During the RCP test, Mix F shows the highest
21 temperature increase (17°C) compared to mix M (9°C) and Mix P (6°C). It was found that for
22 porous concrete, the heating effect will intensify and accelerate the chloride penetration [25].
23 Due to the heating effect, RCP can give erroneously high values especially when poor-quality

concrete is used, and the high values may not truly represent concrete electrical resistivity.

As reported by previous researchers [9], [10], RCP results should linearly correlate with surface resistivity because both methods can give a resistance value when an electrical current passes the specimen. However, that was not the case for most researchers and non-linear fitted curves were mostly established, as shown in Fig.8. Also, if a vertical line is drawn at which RCP value equals 1500, a different phenomenon can be observed on different sides of the line. At RCP values below 1500, the surface resistivity for different materials relatively scatters, but once RCP values pass 1500, all the curves are approaching a horizontal line. This is mainly due to the fact that when surface resistivity dropped to a certain level, the RCP value increased dramatically. Based on the observation, it is speculated that the heating effect is the main cause for non-linearity of the resistivity-RCP relationship, and such effect intensified when RCP passed a certain threshold ($RCP = 1500$).

It is not recommended to correlate RCP and resistivity directly if the binding capability of the materials to chloride ions is unknown. Yet, some measures could be taken to improve the correlation between RCP and resistivity test methods. First, in order to take the binding effect into consideration, the specimens could possibly be immersed to chloride solutions prior to surface resistivity measurements. Additionally, for mitigating the heating effect of RCP test, one-minute RCP test could be an alternative to the traditional RCP test method, as recommended by Julio-Betancourt and Hooton [25].

Relationship Between Mechanical Properties and Electrical Resistivity

For building up the relationship between resistivity and compressive strength, compressive strength is plotted as abscissa while resistivity as the ordinate. As shown in Fig. 8, there is a poor correlation between compressive strength and concrete resistivity ($R^2 = 0.3339$), which agrees with the results reported in other studies [2]. Some work was done to reveal the factors that affect the strength-resistivity relationship. Wedding and Carino [26] improved the accuracy of strength prediction based on resistivity by taking into account the thermal energy release during cement hydration. The success of this improvement in strength prediction in some way indicates the important role of cement hydration in determining the strength-resistivity relationship. Chi et al. [27] have effectively described the microstructure variation by proposing a specific hydration model, and have found the chemical composition and microstructures fundamentally determine the resistivity-strength relationship.

However, some researchers also found a linear correlation between resistivity and compressive strength with a correlation of determination value of 0.9826 [3]. The correlation function was built based on the test results of the same mix design at different curing ages. By analyzing the materials used by other researchers, as summarized in Table 1, it can be found that using similar materials is more likely to achieve a high coefficient of determination. Also, as observed in Fig. 8, Ref [2] and Ref [8] have reported very similar trendlines which may result from the fact that they both use Type I cement, Metakaolin, and similar water/binder (w/b) ratios. In this study, one of the important reasons that a good fit cannot be achieved is because these three repair materials have a large difference in the mix design. Additionally, as shown in Fig. 8, results from this study and all studies have confirmed that high-strength concrete tends to have high resistivity values.

1 In summary, it is not recommended to use resistivity method to predict the compressive
2 strength of the concrete repair. Due to the large difference between different commercial repair
3 product, concrete repair having high resistivity may not always have high strength.

5 **Relationship Between Permeability and Electrical Resistivity**

6 The permeability, as well as the surface resistivity results, of three mixes at 28-day curing ages,
7 are plotted in Fig. 9. A second-order polynomial relationship can be established between
8 resistivity and water permeability results with a coefficient of determination value of 0.8573,
9 which indicates a good correlation. It was reported that both resistivity and compressive
10 strength of materials depend on the pore microstructure [2]. Test results in this study are
11 compared with the trendline from Ramezaniapour et al. [2], and it can be found that concrete
12 repair materials showed superior resistivity performance at the same water penetration depth
13 in comparison to conventional concrete mixes. At 28 days of curing, Mix M possess the lowest
14 water penetration depth followed by Mix F and Mix P. Because Mix P is modified by polymers,
15 it can be observed that the data points of Mix P are a little bit far from Mix M and Mix F, as
16 well as from the fitted curve by Ramezaniapour et al. [2]. It is suspected the relatively less
17 permeable polymer alter the pore microstructure of the concrete and thus may result in reduced
18 water permeability and high resistivity. A similar phenomenon was observed by other
19 researchers as well [28]. Based on the test results in this study, surface resistivity test can
20 provide a reasonable indication of the water permeability in concrete repair.

22 **Relationship Between Surface and Bulk Resistivity**

As shown in Fig. 11, there is a strong linear correlation between surface and bulk electrical resistivity of repair materials with a R^2 value of 0.9975. Each point in Fig. 11 represents each mix at 90 days of curing ages of three repair materials. Average values along with standard deviation for the data presented in Fig. 7, 9, and 11 are summarized in Table 4. In the context of repair materials, the surface resistivity is found to be 2.41 times on average higher than bulk resistivity which is similar to findings from other researchers, i.e., 1.86 (Spragg et al. [29]) and 1.9 (Gudimettla and Crawford [30], Azarsa and Gupta [16]). It was reported that the conversion factor between surface and bulk resistivity depended on the type of materials used and the curing ages [16]. In the past, most researchers found a good correlation between surface and bulk resistivity methods using conventional concrete mixes. This study proves that the good relationship remains unchanged in the context of concrete repairs.

Half-cell Potential Validation

The half-cell potential measurements of two different materials, Mix F and Mix P, with a cover depth of 0.5 and one inch (12.7 and 25 mm) as indicated in parentheses, are summarized in Table 5. The data points are evaluated based on eight measurements across the bottom surface of the specimens closer to the rebar. The average measurement values were adopted here as per ASTM C 876 because the variation between measurements is relatively small (i.e., less than 150mV). As shown in Table 5, the results of Mix F (0.5), Mix F (1), and Mix P (0.5) are more positive than -200mV, which indicates there is a greater than 90% probability that no reinforcing steel occur in the measuring area. The half-cell potential of Mix P (1) is in the range of -200 mV to -350 mV, which indicates the corrosion activity of the reinforcing steel in measuring area is uncertain. From previous results, no clear relationship was found between

cover depth and half-cell potential values. One of the main reasons is that 1-year exposure may not be sufficient for rebars to corrode so that no perceivable difference can be found across different repair materials and specimens with different cover depth.

Durability of Repair Materials

Durability of repair materials defines the remaining service life of the structure and when the next repair should be performed. In this study, cementitious repair mortar (Mix M) shows a good durability performance by having the highest electrical resistivity and relatively low water permeability, and it also possesses the highest compressive strength among the three mixes. Polymer-modified cementitious mortar (Mix P) shows the best resistance to chloride penetration but is inferior in compressive strength, water permeability, and electrical resistivity. Similar findings were reported by Al-Zahrani et al. [31] that polymer-modified materials had lower compressive strength compared to cement-based concrete. Nevertheless, most polymer-modified materials in their study showed higher electrical resistivity, and no difference can be observed between all mixes regarding chloride penetration (ASTM C1202). Lukovic et al. [32] summarized the advantages of both cementitious materials and polymer-modified cementitious materials. It was found that cementitious materials had comparable properties to substrate, low cost, and good resistance to high temperature. In contrast, polymer modified cementitious materials had better mechanical properties, less shrinkage, high early strength, and better resistance to aggressive environment. However, given the vast difference in composition of repair materials, polymer-modified materials may not always have the aforementioned advantages compared to cementitious concrete. In fact, by comparing performance results in this study with those reported by other researchers [31], [33], significant variations can be

observed in durability-related properties of different cement-based and polymer-modified repair materials, and most likely this is caused by the difference in their composition.

In addition, the term ‘durability’ should not be confined to how durable the repair materials are, and in fact, the compatibility between the substrate and the repair is of more importance. And the compatibility is often affected by a wide variety of factors including chemical, electrochemical, permeability, and dimensional compatibility [34], which are beyond the scope of this paper. The future study of this paper will be to study the bonding characteristics of different repair systems under different weathering conditions.

CONCLUSIONS

Based on the experimental study of concrete repair materials using surface/bulk resistivity, RCP, permeability, half-cell potential, and compression test, conclusions can be drawn as shown below:

1. The surface resistivity method shows a strong correlation with the water penetration test, and their relationship can be expressed in the form of a second-order polynomial ($R^2=0.8573$). The surface resistivity demonstrates the capability to provide a reasonable indication of permeability in concrete repairs. Additionally, concrete repair material indicates superior resistivity performance compared with conventional concrete when their water penetration is the same.
2. The surface resistivity indicates a linear correlation with the bulk resistivity test method ($R^2=0.9975$). Previous researchers have found a strong correlation between these two methods using conventional concrete. This study proves that the same trend also applies

1 to concrete repair. Therefore, the two tests can be used interchangeably to evaluate
2 concrete resistivity performance.

- 3 3. Results from RCP test indicate no apparent relationship with concrete resistivity values.
4 This deviation could be caused by the heating effect due to the high voltage imposed
5 on the testing cell and by the different binding capability of different repairs to chloride
6 ions. More research is required to overcome the drawback of RCP method in order to
7 obtain more accurate results.
- 8 4. Compressive strength values show a weak correlation to the resistivity properties of
9 repair materials with a coefficient of determination value of only 0.3399. Therefore, it
10 is not recommended to use resistivity as an indicator for compressive strength.
11 However, in this study, the material with higher resistivity tends to show high
12 compressive strength. The coefficient of determination is expected to increase if
13 materials with similar compositions are used as the subject.
- 14 5. Half-cell potential measurements did not show any difference in materials with
15 different permeability, compressive strength, and electrical conductance properties. A
16 longer immersion time of the specimens in the simulated seawater is recommended in
17 order to get distinctive results.
- 18 6. Surface resistivity may not be used as an alternative to other durability performance test
19 when repair materials are tested as the subject due to the large variation in composition
20 existing in different repair materials.
- 21 7. Compared to cementitious concrete (Mix F) and polymer-modified concrete mortar
22 (Mix P), cementitious concrete mortar (Mix M) show the best durability performance,
23 i.e., low water penetration, high concrete resistivity, and high compressive strength.

However, further tests are required for this material to evaluate its compatibility with the substrate.

ACKNOWLEDGMENTS

Financial support of Natural Sciences and Engineering Research Council of Canada (NSERC) is greatly appreciated. Involvement and guidance of Terry Bergen, Peter Dias, and John Bourcet from Read Jones Christoffersen Ltd is also acknowledged. Previous work done by Shawn Chan is also appreciated. Technical staff Armando Tura and Matt Walker is gratefully acknowledged.

REFERENCES

- [1] “Canadian Infrastructure Report Card 2016 | Federation of Canadian Municipalities.” [Online]. Available: <https://fcm.ca/en/resources/canadian-infrastructure-report-card-2016>. [Accessed: 10-Sep-2019].
- [2] A. A. Ramezani-pour, A. Pilvar, M. Mahdikhani, and F. Moodi, “Practical evaluation of relationship between concrete resistivity, water penetration, rapid chloride penetration and compressive strength,” *Constr. Build. Mater.*, vol. 25, no. 5, pp. 2472–2479, May 2011.
- [3] R. M. Ferreira and S. Jalali, “NDT measurements for the prediction of 28-day compressive strength,” *NDT E Int.*, vol. 43, no. 2, pp. 55–61, Mar. 2010.
- [4] P. Azarsa, R. Gupta, and A. Biparva, “Assessment of self-healing and durability parameters of concretes incorporating crystalline admixtures and Portland Limestone Cement,” *Cem. Concr. Compos.*, vol. 99, pp. 17–31, May 2019.
- [5] A. Lübeck, A. L. G. Gastaldini, D. S. Barin, and H. C. Siqueira, “Compressive strength and electrical properties of concrete with white Portland cement and blast-furnace slag,” *Cem. Concr. Compos.*, vol. 34, no. 3, pp. 392–399, Mar. 2012.
- [6] T. D. Rupnow and P. J. Icenogle, “Surface Resistivity Measurements Evaluated as Alternative to Rapid Chloride Permeability Test for Quality Assurance and Acceptance,” *Transp. Res. Rec. J. Transp. Res. Board*, vol. 2290, no. 1, pp. 30–37, Jan. 2012.
- [7] L. Jackson, “Surface resistivity test evaluation as an Indicator of the Chloride Permeability of Concrete (TechBrief) Publication No. FPIWA-HRT-13-024,” *Public Roads*, vol. 77, no. 1, pp. 47-, 2013.

- [8] A. A. Ramezani-pour and H. Bahrami Jovein, "Influence of metakaolin as supplementary cementing material on strength and durability of concretes," *Constr. Build. Mater.*, vol. 30, pp. 470–479, May 2012.
- [9] H. Layssi, P. Ghods, A. R. Alizadeh, and M. Salehi, "Electrical resistivity of concrete," *Concr. Int.*, vol. 37, no. 5, pp. 41–46, 2015.
- [10] G. A. Julio-Betancourt and R. D. Hooton, "Study of the Joule effect on rapid chloride permeability values and evaluation of related electrical properties of concretes," *Cem. Concr. Res.*, vol. 34, no. 6, pp. 1007–1015, Jun. 2004.
- [11] S. Ahmad, A. K. Azad, and K. F. Loughlin, "Effect of the Key Mixture Parameters on Tortuosity and Permeability of Concrete," *J. Adv. Concr. Technol.*, vol. 10, no. 3, pp. 86–94, Mar. 2012.
- [12] P. Halamickova, R. J. Detwiler, D. P. Bentz, and E. J. Garboczi, "Water permeability and chloride ion diffusion in portland cement mortars: Relationship to sand content and critical pore diameter," *Cem. Concr. Res.*, vol. 25, no. 4, pp. 790–802, May 1995.
- [13] A. Perrot, D. Rangeard, V. Picandet, and S. Serhal, "Effect of coarse particle volume fraction on the hydraulic conductivity of fresh cement based material," *Mater. Struct.*, vol. 48, no. 7, pp. 2291–2297, Jul. 2015.
- [14] D. N. Winslow, M. D. Cohen, D. P. Bentz, K. A. Snyder, and E. J. Garboczi, "Percolation and pore structure in mortars and concrete," *Cem. Concr. Res.*, vol. 24, no. 1, pp. 25–37, Jan. 1994.
- [15] X. Li, Q. Xu, and S. Chen, "An experimental and numerical study on water permeability of concrete," *Constr. Build. Mater.*, vol. 105, pp. 503–510, Feb. 2016.
- [16] P. Azarsa and R. Gupta, "Electrical Resistivity of Concrete for Durability Evaluation: A Review," *Adv. Mater. Sci. Eng.*, vol. 2017, pp. 1–30, 2017.
- [17] ASTM C39 / C39M-18, Standard Test Method for Compressive Strength of Cylindrical Concrete Specimens, ASTM International, West Conshohocken, PA, 2018, www.astm.org.
- [18] T. AASHTO, "95,(2011),", *Stand. Method Test Surf. Resist. Indic. Concr. Abil. Resist Chloride Ion Penetration*.
- [19] ASTM C1760-12, Standard Test Method for Bulk Electrical Conductivity of Hardened Concrete, ASTM International, West Conshohocken, PA, 2012, www.astm.org.
- [20] ASTM C1202-17a, Standard Test Method for Electrical Indication of Concrete's Ability to Resist Chloride Ion Penetration, ASTM International, West Conshohocken, PA, 2017, www.astm.org.
- [21] Boyu Wang, Rishi Gupta, Peter Dias, Terry Bergen, "Coefficient of permeability of cement-based repair materials ,", 1st International Conference on New Horizons in Civil Engineering, April 25-27, 2018, Victoria, Canada.
- [22] ASTM C876-15, Standard Test Method for Corrosion Potentials of Uncoated Reinforcing Steel in Concrete, ASTM International, West Conshohocken, PA, 2015, www.astm.org.
- [23] S. Mindess, J. F. Young, and D. Darwin, *Concrete*, 2nd ed. Upper Saddle River, NJ: Prentice Hall, 2003.
- [24] Q. Yuan, C. Shi, G. De Schutter, K. Audenaert, and D. Deng, "Chloride binding of cement-based materials subjected to external chloride environment – A review," *Constr. Build. Mater.*, vol. 23, no. 1, pp. 1–13, Jan. 2009.
- [25] G. A. Julio-Betancourt and R. D. Hooton, "Study of the Joule effect on rapid chloride permeability values and evaluation of related electrical properties of concretes," *Cem. Concr. Res.*, vol. 34, no. 6, pp. 1007–1015, Jun. 2004.

- [26] P. Wedding and N. Carino, "The Maturity Method: Theory and Application," *Cem. Concr. Aggreg.*, vol. 6, no. 2, p. 61, 1984.
- [27] L. Chi, Z. Wang, S. Lu, D. Zhao, and Y. Yao, "Development of mathematical models for predicting the compressive strength and hydration process using the EIS impedance of cementitious materials," *Constr. Build. Mater.*, vol. 208, pp. 659–668, May 2019.
- [28] F. Moodi, A. Kashi, A. A. Ramezaniapour, and M. Pourebrahimi, "Investigation on mechanical and durability properties of polymer and latex-modified concretes," *Constr. Build. Mater.*, vol. 191, pp. 145–154, Dec. 2018.
- [29] R. P. Spragg, J. Castro, T. Nantung, M. Paredes, and J. Weiss, "Variability analysis of the bulk resistivity measured using concrete cylinders," *Adv. Civ. Eng. Mater.*, vol. 1, no. 1, pp. 1–17, 2012.
- [30] J. Gudimettla and G. Crawford, "Resistivity Tests for Concrete—Recent Field Experience," *ACI Mater. J.*, vol. 113, no. 4, 2016.
- [31] M. M. Al-Zahrani, M. Maslehuddin, S. U. Al-Dulaijan, and M. Ibrahim, "Mechanical properties and durability characteristics of polymer- and cement-based repair materials," *Cem. Concr. Compos.*, vol. 25, no. 4, pp. 527–537, May 2003.
- [32] M. Lukovic, G. Ye, and K. Van Breugel, "Reliable concrete repair: A critical review," *14th Int. Conf. Struct. Faults Repair Edinb. Scotl. UK 3-5 July 2012*, 2012.
- [33] J. Cabrera and A. Al-Hasan, "Performance properties of concrete repair materials," *Constr. Build. Mater.*, vol. 11, no. 5, pp. 283–290, Jan. 1997.
- [34] D. R. Morgan, "Compatibility of concrete repair materials and systems," *Constr. Build. Mater.*, vol. 10, no. 1, pp. 57–67, Feb. 1996.
- [35] M. Ibrahim and M. Issa, "Evaluation of chloride and water penetration in concrete with cement containing limestone and IPA," *Constr. Build. Mater.*, vol. 129, pp. 278–288, Dec. 2016.
- [36] J. Wongpa, K. Kiattikomol, C. Jaturapitakkul, and P. Chindaprasirt, "Compressive strength, modulus of elasticity, and water permeability of inorganic polymer concrete," *Mater. Des.*, vol. 31, no. 10, pp. 4748–4754, Dec. 2010.

APPENDIX

Abbreviations

- RCP: Rapid Chloride Permeability
- CON: Concrete
- CEM: Cement paste
- MOR: Mortar
- SF: Silica Fume
- RHA: Rice Husk Ash
- OPC: Ordinary Portland Cement
- w/b: Water/binder ratio
- PLC: Portland Limestone Cement
- PC: Portland Cement
- GGBS: Ground Granulated Blast-furnace Slag
- Comp: Compressive strength
- WP: Water Penetration
- WPD: Water Penetration Depth (unit: mm)
- WPC: Water Permeability Coefficient (unit: m/s)
- RHBA: Rice husk–bark ash
- ITZ: Interfacial Transition Zone
- w/m: Water/material ratio
- ppt: particle per thousand
- SSD: Saturated Surface Dry
- SR: Surface Resistivity
- BR: Bulk Resistivity

- 1 WP: Water Penetration
- 2 SEM: Scanning Electron Microscope
- 3 EDX: Energy-dispersive X-ray spectroscopy
- 4 Avg. Average value
- 5 SD: Standard Deviation
- 6
- 7
- 8
- 9
- 10
- 11
- 12
- 13
- 14
- 15
- 16
- 17
- 18
- 19
- 20
- 21
- 22
- 23

TABLES AND FIGURES

List of Tables:

Table 1 – Empirical relationship between different test methods

Table 2 – Repair materials information

Table 3 – Curing ages of all specimens

Table 4 – Summary of statistical data shown in graphs

Table 5 – Average half-cell potential measurements on prism specimens (after one year)

1 **List of Figures:**

2

3 **Fig. 1** – Surface resistivity test (a) apparatus schematic (b) Giatec SurfTM test setup

Fig. 2 – Bulk resistivity test (a) apparatus schematic (b) Giatec RCON2TM test apparatus

Fig. 3 – RCP test setup

Fig. 4 – Water penetration test (a) permeability test apparatus located in Facility for Innovative Materials & Infrastructure Monitoring (FIMIM) (b) Forney compressive test machine

Fig. 5 – Outline of penetration depth

Fig. 6 – Half-cell potential measurements on slabs reinforced with rebar (red) (all dimensions are in mm)

Fig. 7 – Correlation between RCP and surface resistivity (in this study vs. other literature)

Fig. 8 – Correlation between compressive strength and surface resistivity (in this study vs. other literature)

Fig. 9 – Correlation between permeability and concrete resistivity (in this study vs. other literature)

Fig. 10 – (a) Surface resistivity over ages (b) Compressive strength over ages

Fig. 11 – Correlation between surface and bulk resistivity

Table 1 Empirical relationship between different test methods

Ref.	Methods	Empirical relationship	R^2	w/b	Composition
[2]	RCP (x) vs. SR (y)	$y = 67998x^{-1.028}$	0.8977	0.4,0.45,0.5,0.	Type I cement, RHA, Tuff,
				55,0.6	Pumice, Silica fume,
[4]	RCP (x) vs. SR (y)	$y = -12.2 \times 10^{-4}x + 10.72$	0.43	0.532	Type I OPC, type GUL PLC
[8]	RCP (y) vs. SR (x)	$y = 6454.4e^{-0.04x}$	0.9219	0.35,0.4,0.5	Type I cement, Metakaolin
[7]	RCP (y) vs. SR (x)	$y = 98441x^{-1.35}$	0.92	0.37,0.42,0.45, 0.47	Type I/II cement, fly ash, limestone powder
[6]	RCP (y) vs. SR (x)	$y = 29647x^{-0.944}$	0.8922	0.35,0.5,0.65	Type I/II cement, fly ash, slag, silica fume
[2]	Comp (x) vs. SR (y)	$y = 0.0196x^2 - 1.0519x + 25.776$	0.4131	0.4,0.45,0.5,0.	Type I cement, RHA, Tuff,
[8]	Comp (x) vs. SR (y)	$y = 4.4839e^{0.0331x}$	0.843	55,0.6 0.35,0.4,0.5	Pumice, Silica fume, Type I cement, Metakaolin

Table 1 Continued

Ref	Methods	Empirical relationship	R^2	w/b	Material constituents
[3]	Comp (x) vs. SR (y)	$y = 0.5654x + 4.3608$	0.9675	0.5	Type I OPC
[3]	Comp (x) vs. SR (y)	$y = 0.0464x + 25.911$	0.9826	0.4	Type IV cement and fly ash
[5]	Comp (y) vs. SR (x)	Linear	-	0.3,0.42,0.55	White PC, high early strength PC, GGBS
[2]	WPD (x) vs. SR (y)	$y = 107.88x^{-0.777}$	0.8268	0.4,0.45,0.5,0	Type I cement, RHA, Tuff, Pumice, Silica
				.55,0.6	fume, Metakaolin
[35]	RCP (x) vs. WPD (y)	Parabola	0.86	0.4,0.42,0.44	Type I cement, fly ash, GGBS, Limestone, inorganic process additions
[36]	Comp (x) vs. WPC (y)	$y = (1.659 \times 10^{-11})x^{-1.146}$	-	-	Fly ash, RHBA, sodium silicate, sodium hydroxide

1 **Table 2 Repair materials information**

Material	Category	Aggregate	w/m	Density, kg/m^3	Slump, mm (inch)	Setting time	Air content
Mix F	Cementitious repair concrete	Coarse with max. size 10 mm (0.39inch)	10%	2383.4	80 (3.1)	-	1.7%
Mix M	Cementitious repair mortar	Sand	8%	2335.2	70 (2.8)	75 min	1.6%
Mix P	Polymer- modified cementitious repair mortar	None	17%	2092.1	15 (0.6)	9 min	3.6%

2

1 **Table 3—Curing time of all specimens**

Mixes	Test ages (in days)					
	RCP	SR	BR	WP	Comp	H.C
F	28	28; 42; 56; 70; 70(14); 70(28)	90	28	1; 3; 7; 28; 70; 70 (14)	365*
M	28	28; 42; 56; 70; 70(14); 70(28)	90	28	1; 3; 7; 28; 70; 70(14)	—
P	28	28; 42; 56; 70; 70(14); 70(28)	90	28	1; 3; 7; 28; 70; 70(14)	365*

*All numbers under test ages indicate the days immersed in tap water at ambient temperature ($23 \pm 2^{\circ}\text{C}$) unless otherwise stated.

*The number in parenthesis indicate the additional days of chloride immersion in simulated seawater at $23 \pm 2^{\circ}\text{C}$.

*The asterisk means special treatment which includes a 70-day tap water (at $23 \pm 2^{\circ}\text{C}$) immersion, a 28-day simulated seawater immersion ($23 \pm 2^{\circ}\text{C}$), a 14-day simulated seawater immersion at 60°C , and exposure to open space until it reaches one-year old

1 **Table 4 Summary of statistical data shown in graphs**

	Unit	Mix F		Mix M		Mix P	
		Avg.	SD	Avg.	SD	Avg.	SD
RCP (Fig. 7)	Coulomb	2802.7	66.9	1396.8	17.3	749.8	71.2
SR (Fig. 7)	$k\Omega \cdot cm$	58.8	1.6	50.7	1.7	38.4	2.5
WPD (Fig. 9)	mm	14	0.9	8.2	2.5	51.5	21.8
	(inch)	(0.6)	(0.04)	(0.3)	(0.02)	(2)	(0.9)
SR (Fig. 9)	$k\Omega \cdot cm$	58.3	1.0	57.3	0.8	38.7	4.0
BR (Fig. 11)	$k\Omega \cdot cm$	14.6	0.8	53.0	2.7	30.4	2.4
SR (Fig. 11)	$k\Omega \cdot cm$	28.0	1.4	120.3	6.7	62.9	4.9

2 **Table 5—Average half-cell potential measurements on prism specimens (after one year)**

Position	1	2	3	4	5	6	7	8	Avg. (mV)
Mix F (0.5)	-89	-85	-84.3	-82	-82	-79	-76	-72	-81
Mix F (1)	-133	-123	-158	-206	-196	-154	-125	-136	-154
Mix P (0.5)	-235	-106	-138	-171	-185	-139	-145	-167	-161
Mix P (1)	-240	-243	-233	-251	-244	-231	-225	-234	-238

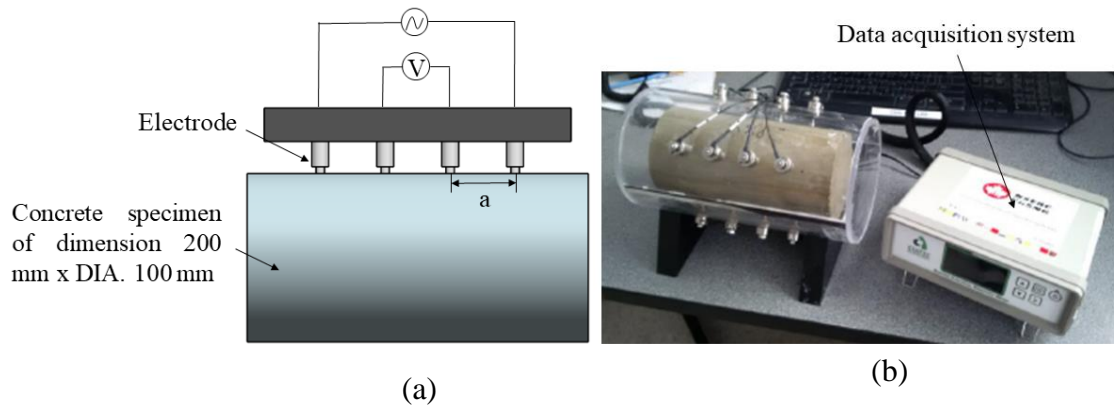


Fig. 1—Surface resistivity test (a) apparatus schematic (b) Giatec Surf™ test setup

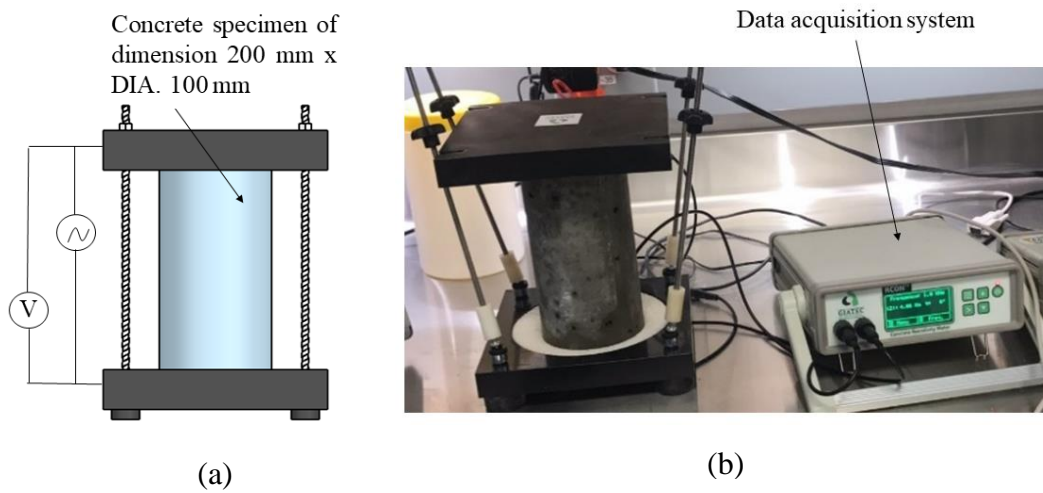


Fig. 2—Bulk resistivity test (a) apparatus schematic (b) Giatec RCON2™ test apparatus

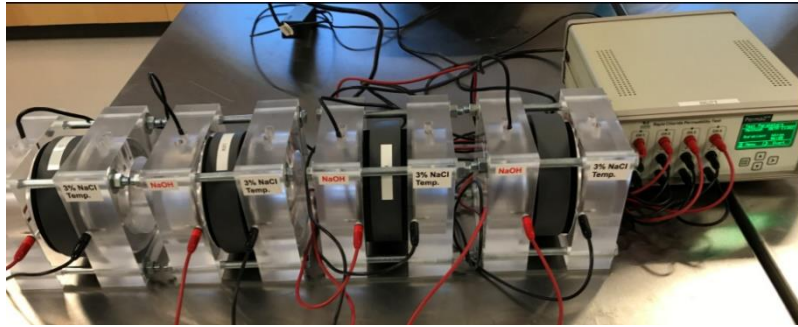
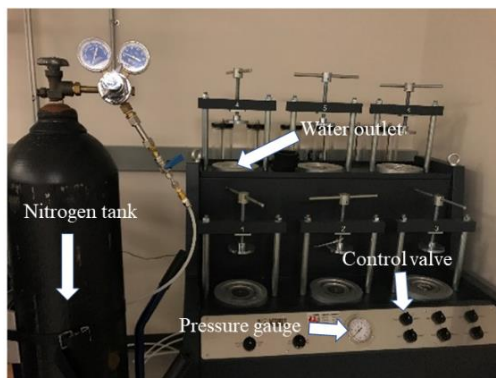
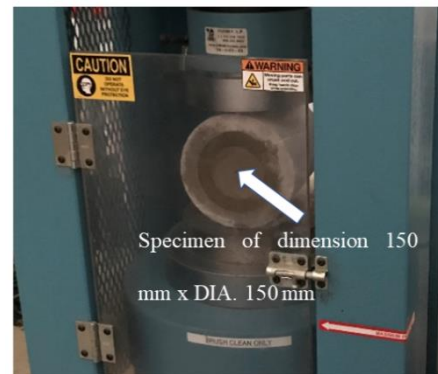


Fig. 3–RCP test setup



(a)



(b)

Fig. 4–Water penetration test (a) permeability test apparatus located in Facility for Innovative Materials & Infrastructure Monitoring (FIMIM) (b) Forney compressive test machine

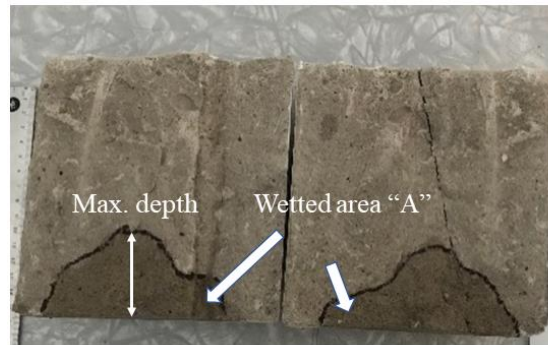
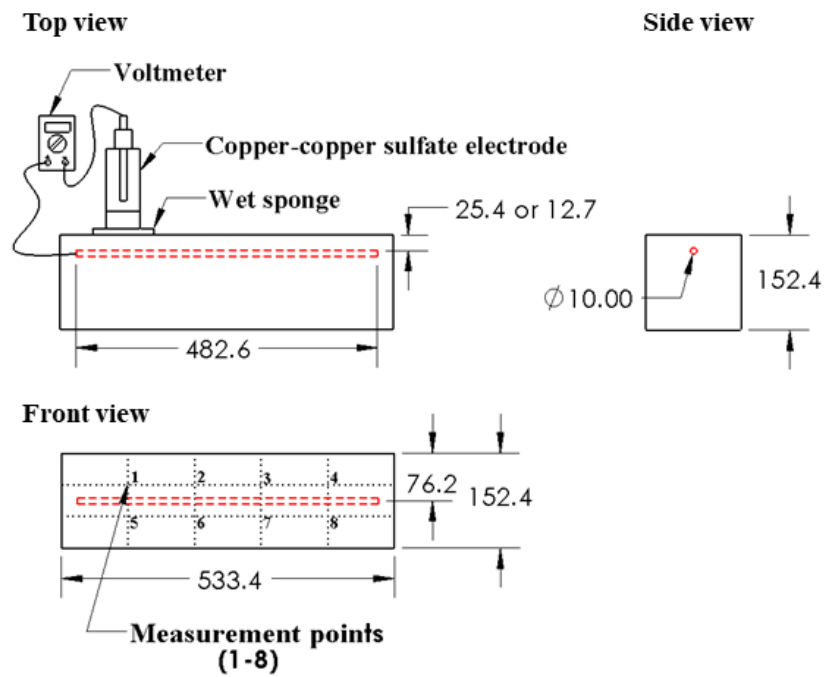


Fig. 5–Outline of penetration depth



1 Fig. 6–Half-cell potential measurements on slabs reinforced with rebar (red) (all dimensions are in
2 mm)

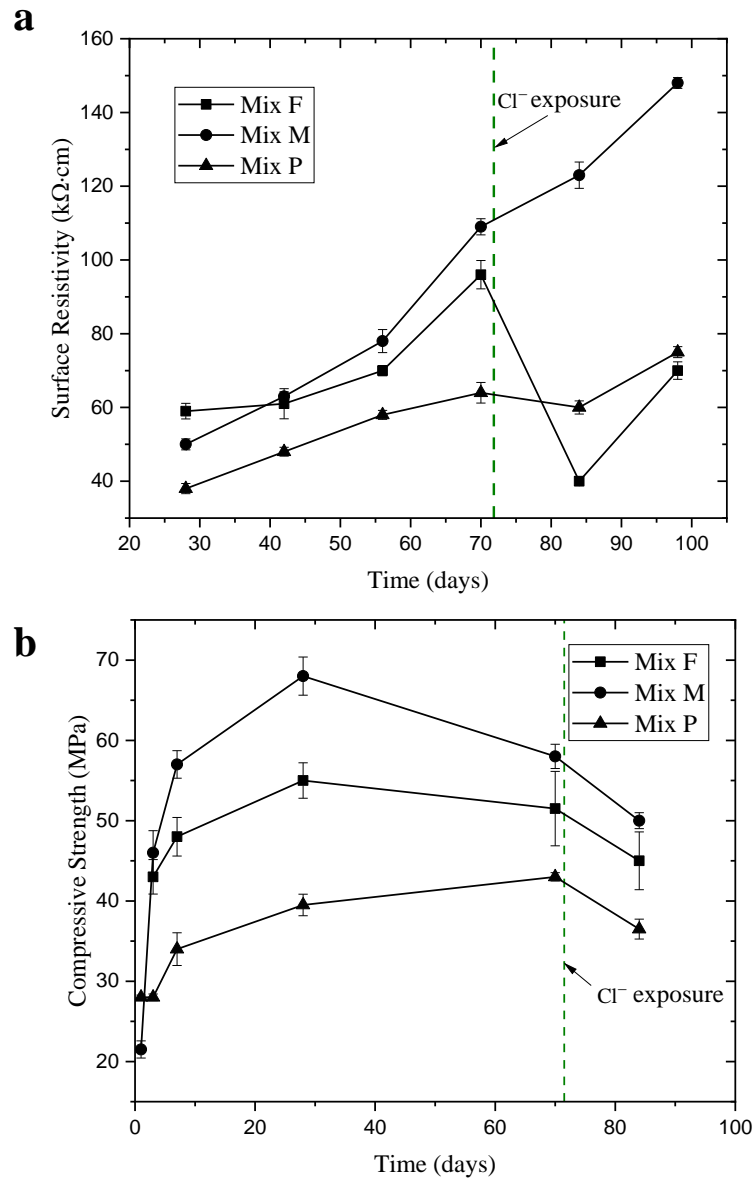


Fig. 7– (a) Surface resistivity over ages (b) Compressive strength over ages

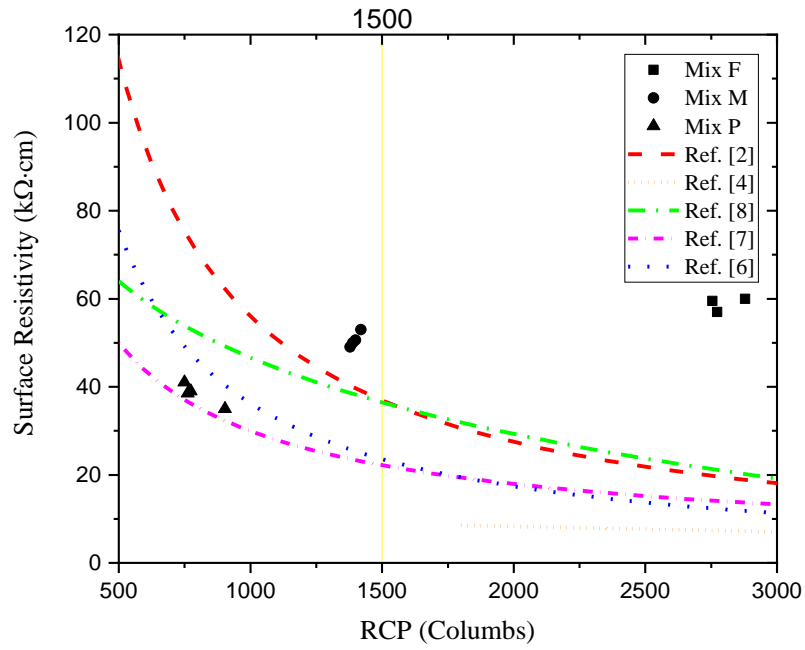


Fig. 8– Correlation between RCP and surface resistivity (in this study vs. other literature)

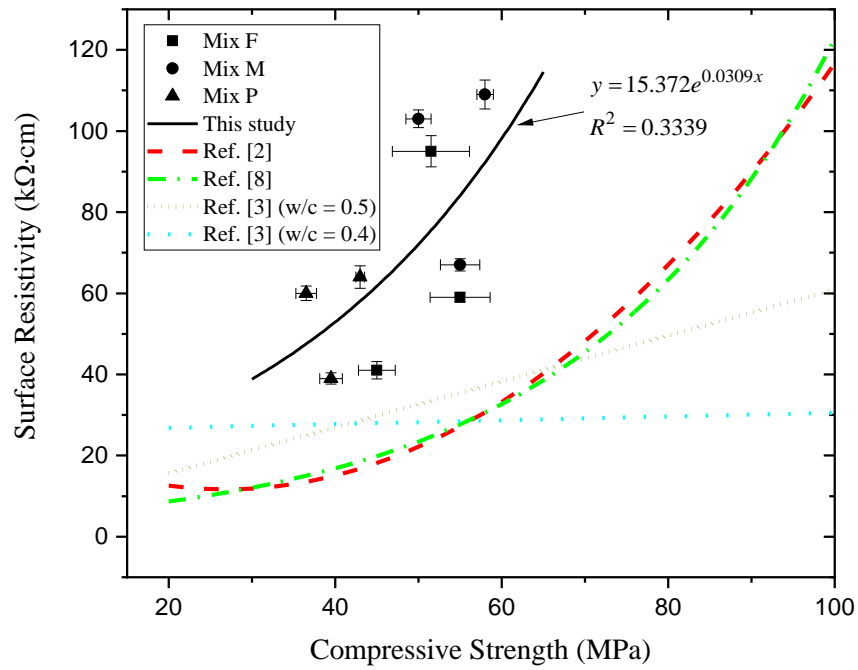


Fig. 9–Correlation between compressive strength and surface resistivity (in this study vs. other literature)

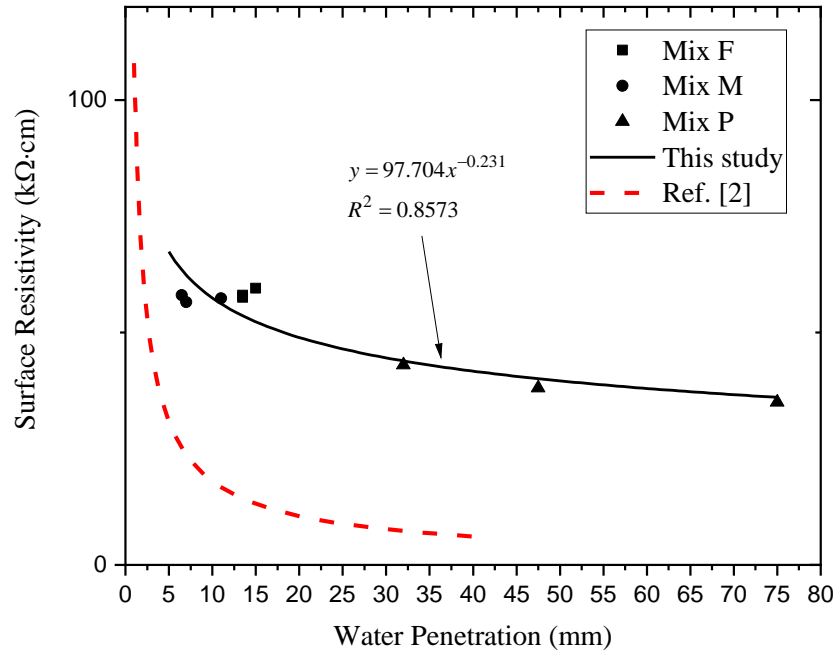


Fig. 10—Correlation between permeability and concrete resistivity (in this study vs. other literature)

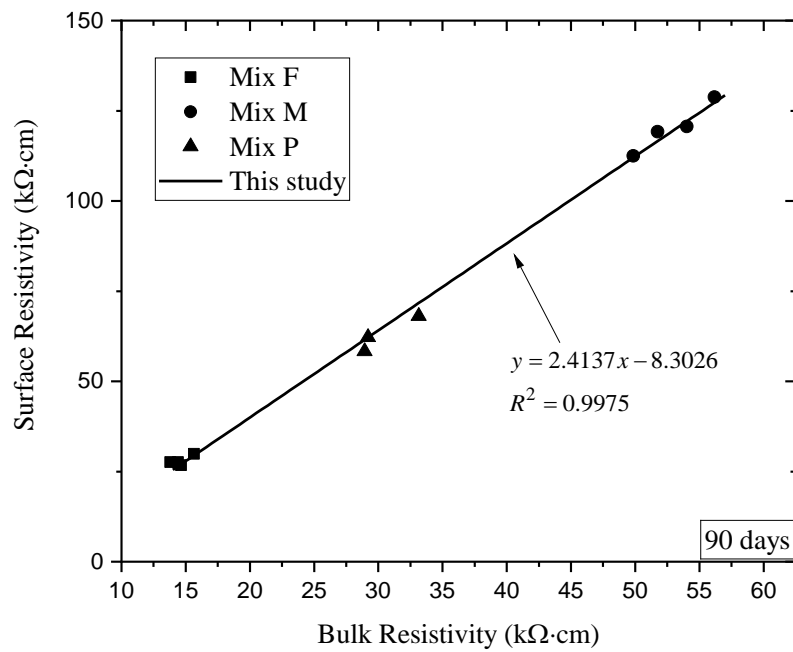


Fig. 11—Correlation between surface and bulk resistivity